

Investigation of the Binding Specificity of Wild Type Human Platelet Profilin
for Phosphatidylinositol-4,5-bisphosphate (PIP₂) and Analogues

Nichole Stewart

Work completed under the supervision of Dr. Martha Oakley.

Submitted to the faculty of the University Graduate School
in partial fulfillment of the requirements
for C500
in the Department of Chemistry,
Indiana University
April 21, 2006

Table of Contents

Objective
3

Introduction
3

Materials and Methods
8

Results and Discussion
13

Conclusions and Future Work
23

References
25

Objective

Protein-lipid interactions mediate many essential cellular functions. Though these interactions are common, very little is known about the specific determinants modulating these interactions. To help better understand the specific requirements of these binding events, we are employing the use of synthetic micelle mimics. The goal of this C500 project was to examine the binding affinity of human profilin I and a branched polymer with 52 PIP₂ headgroups. Additionally, a biotinylated branched polymer with 7 PIP₂ headgroups has been constructed to be used in subsequent binding studies.

Introduction

Phospholipids are crucial components of cellular membranes. One particular type found is phosphoinositides (PIP_n). These lipids are composed of an inositol headgroup, a glycerol backbone, and two fatty acid chains (typically stearic and arachidonic acid) (Figure 1)¹. The inositol headgroup displays five hydroxyl groups which can potentially be phosphorylated. Many variations of phosphoinositides are present in the cellular membrane including PI(3)P, PI(4)P, PI(5)P, PI(3,4)P₂, PI(3,5)P₂, PI(4,5)P₂, and PI(3,4,5)P₃. These are interconverted by kinases and phosphatases depending on cell needs for various signal transduction pathways¹. Processes such as membrane targeting, channel gating for release of intracellular calcium, G protein activation, endocytosis, apoptosis, and cell growth and motility are regulated by phosphoinositides (Figure 1)^{2,3}. Phosphatidylinositol-4,5-bisphosphate (PIP₂), the most abundant phosphoinositide, constitutes approximately 1% of all lipids in the plasma membrane^{4,5}. Cleavage by phospholipase C yields the important second messengers inositol (3,4,5) triphosphate (IP₃) and diacylglycerol (Figure 1). Though PIP₂ is essential for many cellular functions, little is known about the mechanism of its interactions.

Along with having many functions, PIP₂ is recognized by numerous binding domains including PH, PX, FERM, ANTH, ENTH, Tubby, and MARCKS^{6,7}. These domains are structurally diverse, yet all bind to PIP₂ and other phosphoinositides. For example, PH domains, one of the most commonly found, are highly involved with signaling and cytoskeletal functions and contain clusters of basic residues thought to be

involved with binding⁸. A second example is the FERM domain which is characterized by a cloverleaf shape composed of three domains and functions mainly as cross-linkers for the membrane to actin filaments. Crystallographic studies suggest that PIP₂ binds in a basic cleft between two of the subunits⁶. Yet another example is the ENTH domain which is important for membrane remodeling. Binding by PIP₂ causes a conformational change in the N terminus, creating a helix involved with membrane insertion⁶. The involvement with so many different structural features shows the need to understand these interactions on a more detailed level.

PIP₂ also plays a major role in the regulation of the actin cytoskeleton through interactions with key regulating proteins such as WASP-SCAR, gelsolin, cofilin, and profilin³. The conversion of globular ATP-actin to filamentous ADP-actin is mediated through interactions with these proteins. PIP₂ aids with both promotion and prevention of actin polymerization³. One of the better characterized PIP₂ binding partners is profilin, a

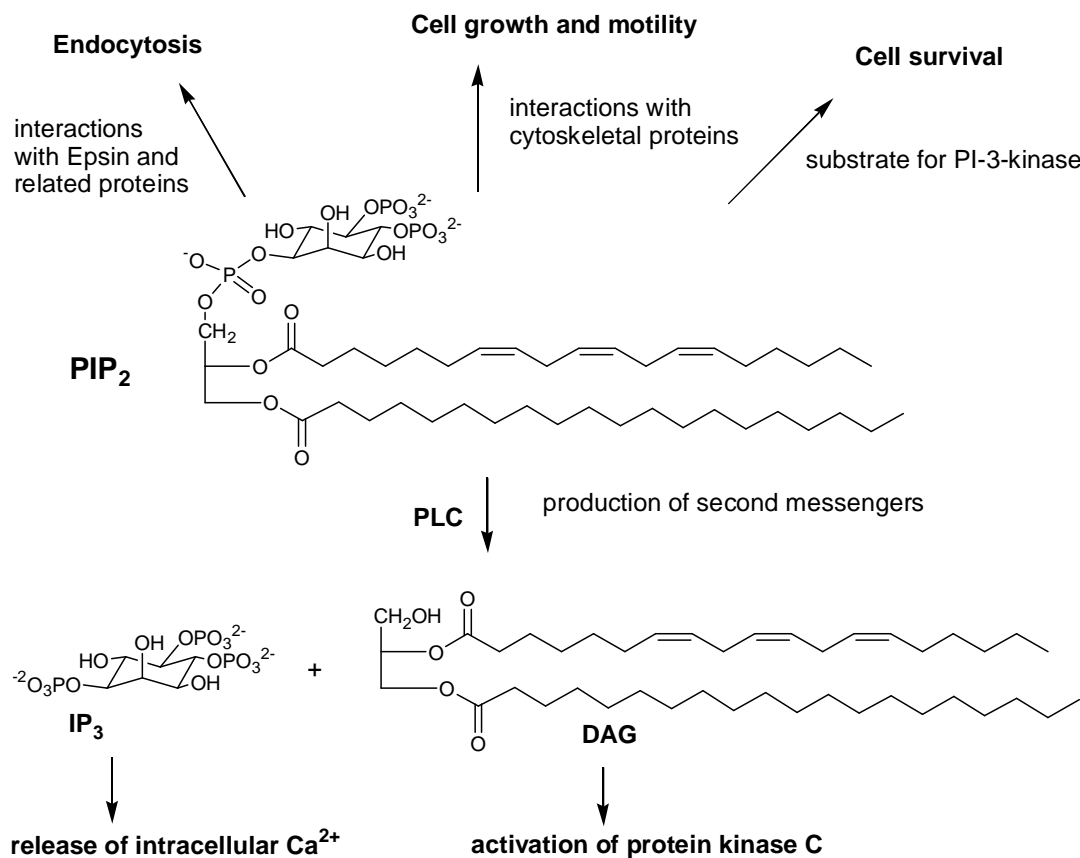


Figure 1. The structure and importance of phosphoinositides in the cell. Figure adapted from thesis of S.A. Webb⁹.

15 kDa globular protein. This protein is found as both a peripheral membrane and cytosolic protein¹⁰. Like PIP₂, it can either act to promote or inhibit actin polymerization¹¹. These interactions play a role in cytoskeletal arrangement and cellular motility. Improper functioning and low levels of profilin can lead to tumor formation¹². Therefore, properly understanding these interactions and pathways may play a crucial role in treatments and cures.

Though profilin is well characterized, its binding sites for PIP₂ are not agreed on. There is evidence for several binding sites for PIP₂ on profilin. One potential site is Arg 88 which was implicated through mutagenesis studies¹³, while another site is Arg 135 and 136. Photoaffinity labels along with computer modeling were used to elucidate this site¹⁴. Generally the binding sites are thought to be located in a highly basic region of the protein potentially close to the terminal ends (Figure 2)¹⁴⁻¹⁷. Evidence also suggests that the PIP₂ and actin binding sites overlap¹⁸. This would account for the experimental data which shows PIP₂ and actin compete for binding with profilin¹⁸. Upon binding with PIP₂, profilin no longer can bind to actin. Experimental evidence suggests that PIP₂ binds to profilin in a multivalent manner. Gel filtration studies indicate that PIP₂ and profilin bind in a 5:1 ratio respectively¹⁹. Though profilin binds to PIP₂, experimental data suggests

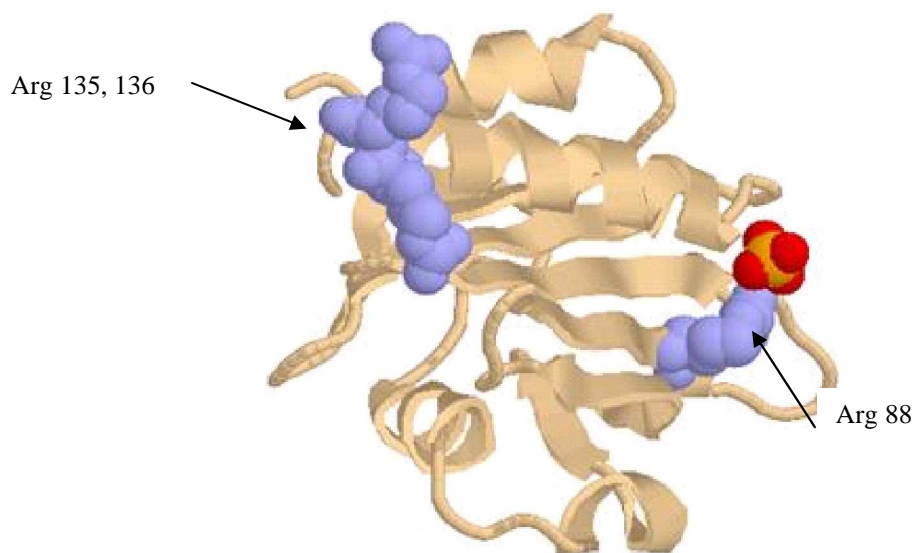


Figure 2. The structure of human profilin I. Residues implicated in binding are shown in purple. A phosphate molecule is indicated in orange and red and was crystallized with the protein. Figure prepared in protein explorer using 1FIK.

that it does not bind to its hydrolysis product IP_3 ²⁰, suggesting that the interaction with only one polar headgroup is not sufficient for binding to occur. Additionally, it has been shown that high salt buffer dissociates the profilin PIP_2 interaction and upon profilin binding to PIP_2 , there is no gross disruption of micellar structure^{10,20}. This data suggest a multivalent binding mechanism. Though it is not clear or agreed upon by others, our hypothesis is that multivalency is essential for the binding mechanism between PIP_2 and profilin. Potentially, more than one PIP_2 molecule is needed for recognition by profilin (Figure 3). Multivalency is not an uncommon method of recognition as there are many examples relevant to human biology. For example, influenza and *E.Coli* both adhere to cell surfaces through multivalent recognition²¹. Additionally neutrophils respond to inflammation in a similar manner²¹. Yet another example involves the multivalent binding of certain transcription factors to DNA²¹.

One way to study this multivalent interaction is by the use of PIP_2 reconstituted in micelles or vesicles. However, this presents several problems. Membrane-like environments such as micelles or vesicles are highly dynamic and fluid. With so much freedom in movement, it would be hard to decipher the orientation and arrangement of

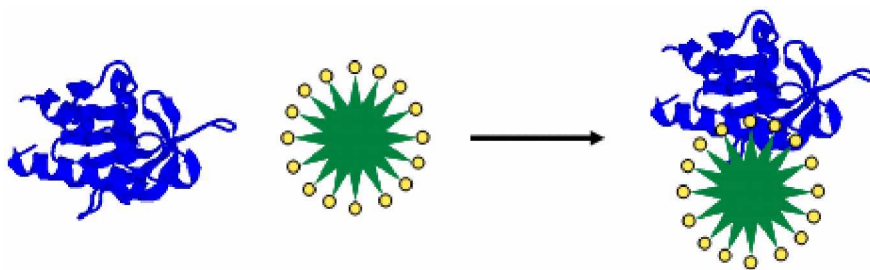


Figure 3. Schematic representation of multivalent interaction between profilin and PIP_2 . Figure shows profilin in blue binding to a micelle of PIP_2 with headgroups shown in yellow and lipid tails in green. It can be seen that multiple headgroups are binding to profilin in the right portion of the figure.

the PIP_2 headgroups upon binding to profilin. One way to circumvent this problem is through the use of a covalent scaffold of PIP_2 molecules. Synthetic multivalent representations of molecules have been documented in the literature including multivalent carbohydrate ligands showing shiga toxin inhibition and multivalent saccharide dendrimers proficient in glycoside clustering^{22,23}.

We have initiated a plan for investigating the PIP₂ profilin interaction by using modified PAMAM dendrimers²⁴. By using a commercially available core and a linker moiety, synthetic PIP₂ headgroups have been covalently attached to the termini (Figure 4). The initial work was carried out in the Oakley lab by Sarah A. Webb⁹, in which she determined a squarate linker to be the most efficient coupling reagent for the PIP₂ headgroup. Much of her work also focused on the order of the chemistry and the synthesis of the PIP₂ headgroup. This synthetic PIP₂ micelle mimic will allow for more control over the spatial arrangement and number of PIP₂ headgroups presented than in a natural micelle or vesicle. Shown in Figure 4 is a generation 0 (G0) micelle mimic with 4 termini. Larger dendrimers have also been synthesized in the lab including G1 (8 headgroups) and G4 (~52 headgroups)²⁵.

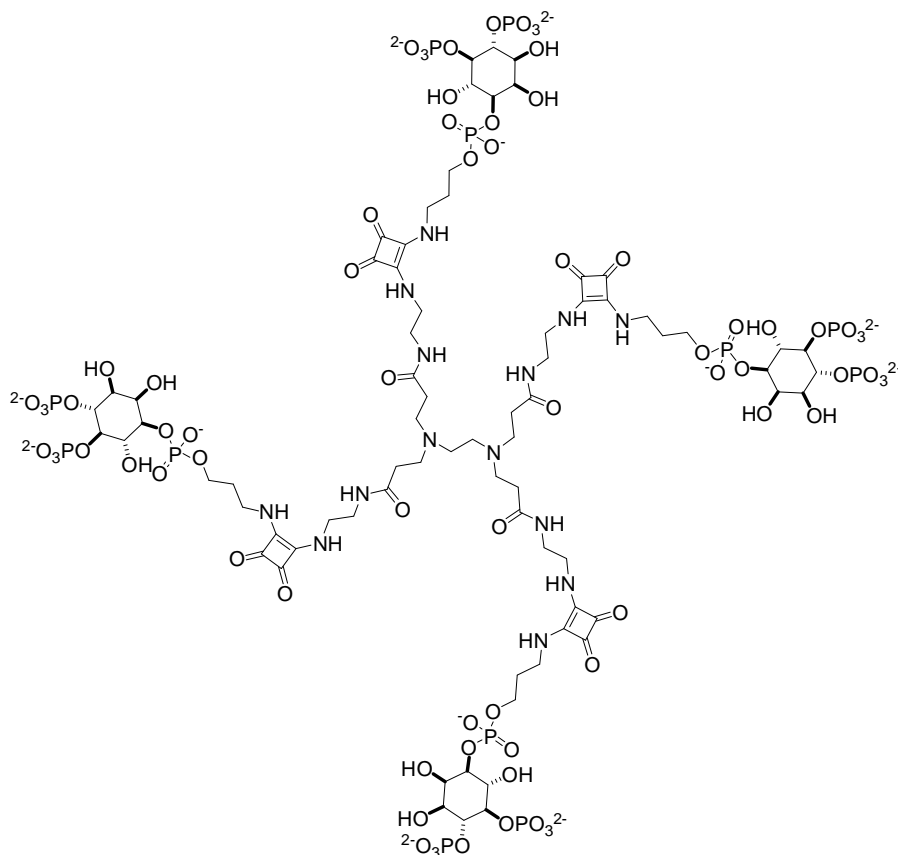


Figure 4. Synthetic PIP₂ generation 0 micelle mimic.

With initial synthetic challenges met, we are currently working on synthesizing variations of the PIP₂ dendrimer and methods of binding to examine the interaction with

profilin. Our goal is to characterize the binding interaction and test whether multivalency is important for binding. From this information, we will be able to compare the binding of the natural substrate PIP₂ and IP₃ to that of the synthetic micelle mimics. Our expectation is that the dendrimers will bind as well as PIP₂ and better than IP₃. However, since the required arrangement of PIP₂ headgroups for binding is unclear, it may take several iterations to achieve binding as tight as that of the natural substrate PIP₂. This will give us an insight as to what is required for selective binding to profilin. Ideally, this information should allow us to design dendrimers which bind specifically to profilin and thus can be used for biological studies. Here, I will present the synthesis of a biotinylated G1 PIP₂ micelle mimic and also the various binding methods that are being used the interaction of a G4 PIP₂ micelle mimic with profilin.

Materials and Methods

Wild Type Protein Expression and Purification

Wild type human profilin was expressed using a T7 bacteriophage expression system²⁶. Briefly, 50µL of BL21(DE3) *E.coli* cells were placed on ice to thaw for 10 minutes. Next, 2-3 µL of the plasmid containing the pMW172 HPP gene were added to the cells and allowed to sit on ice for 30 minutes. Next the cells were heat shocked at 42°C for 45 seconds and immediately placed on ice again for a few minutes. After adding 250 µL of SOC medium, 200 uL were plated on ampicillin plates (100 µg/mL). The plates were grown up overnight at 37°C. Cultures were inoculated from a single colony. After growing overnight (12-16 hours) at 37°C and 225 rpm, the 4 mL of cells were added to a larger culture of 700 mL LB and 700 µL of ampicillin. The cultures were incubated with shaking at 225 rpm for 10-16 hours at 37°C and then harvested by centrifugation at 5000 rpm for 15 minutes in a JA-10 rotor. Next the cells were resuspended in 12 mL of buffer A (10 mM Tris, 40 mM KCl, 1 mM BME pH 7.4). To this, 100 µL of DNase (10 mg/mL) in 100 mM MgCl₂ and 100 µL of PMSF were added. The cells were then lysed by sonication using a 10 minute cycle of 30 seconds on/30 seconds off. This was followed by centrifugation for 15 minutes at 12,000 rpm in a JA-20 rotor. The supernatant was collected for later analysis and the pellet was resuspended in another 12 mL of buffer A.

The sonication procedure was then repeated. Next the supernatants collected were loaded onto a poly-*L*-proline affinity column equilibrated in buffer A at 4°C. First the column was washed with 60 mL of buffer A and then 120 mL of buffer A with 3 M urea. Then the column was allowed to warm to room temperature and the protein was eluted with 60 mL of buffer A with 8 M urea. The fractions collected were analyzed by SDS-PAGE using a polyacrylamide gel composed of 16% resolving gel and 5% stacking gel. A polypeptide molecular weight marker from Bio-Rad was used to identify fractions containing profilin. These fractions were then pooled and concentrated using Amicon centrifugation tubes (1000 MWCO). The samples were subjected to centrifugation at 3000 rpm in the JA-10 rotor for four hours. Next the sample was dialyzed in degassed buffer A in a 1000 MWCO dialysis tube for 4-5 hours with 1-2 buffer changes. The purified protein was then analyzed by SDS-PAGE and MALDI-TOF mass spectrometry.

HTN Profilin Expression and Purification

To express WT profilin with an N-terminal his tag, the pMW172 HPP gene was cloned into a pET-28a(+) vector. First a reaction was set up with 3.5 µL pET-28a(+), 4.0 µL of pMW172 HPP, 2 µL Eco R1 10x buffer, 1 µL of both EcoR1 and Nde1 restriction enzymes, and 8.5 µL of ddH₂O. The reaction was incubated at 37°C overnight. The next day the DNA was ligated back together by adding the following to the reaction: 1 µL DNA ligase, 2 µL T4 DNA ligase buffer, and 0.2 µL 100 mM dATP. The reaction was incubated for 1 hour at room temperature. Afterwards, the ligase was deactivated by heating the reaction to 65°C for 10 minutes. The ligation product was subjected to digestion using the restriction enzyme BamH1 to cleave any remaining original pET vector. The DNA was then transformed using the same procedure as in the previous section except kanomycin plates were used. Sequencing of the plasmid DNA isolated from a single colony of transformed confirmed that the protein did in fact have the N-terminal his tag. The protein was expressed using the same procedure as above. After harvesting the cells, 3.8g of pellet were resuspended in 20 mL of lysis buffer containing 50 mM NaH₂PO₄, 300 mM NaCl, and 10 mM imidazole, pH 8.0. PMSF and DNase were also added and the cells were sonicated as above. The protein was then purified using a

Ni-NTA column at 4°C. The column was equilibrated with 5 column volumes of lysis buffer and the lysate was loaded onto the column. The column was washed with 75 mL buffer containing 50 mM NaH₂PO₄, 300 mM NaCl, and 20 mM imidazole, pH 8.0. Next the protein was eluted with the same buffer, but containing 250 mM imidazole. The fractions were analyzed for protein using SDS-PAGE and then combined and dialyzed into degassed buffer A using 1000 MWCO dialysis tubing for 4-5 hours with 1-2 buffer changes. As above, the purified protein was then analyzed by SDS-PAGE and MALDI-TOF mass spectrometry.

Surface Plasmon Resonance (SPR) Experiments

SPR binding experiments were carried out using a BIAcore 3000. The WT profilin was covalently attached to a CM4 chip using a 4:1 mixture of 0.12 M *N*-hydroxysuccinimide (NHS) and 0.39 M *N*-ethyl-*N'*-(dimethyl-aminopropyl)carbodiimide hydrochloride (EDC) at 20°C. Buffer and pH studies with the protein indicated sodium acetate pH 5.0 to be the most appropriate coupling buffer. Therefore, the protein was dialyzed into this buffer prior to all BIAcore experiments. An attempt to couple the PIP₂ headgroup was carried out in the same way according to the procedure of Prestwich²⁷. The N-terminal his tagged protein was immobilized to the surface of an NTA chip at 4°C. The chip was first activated with Ni²⁺ followed by injection of the protein. Micelles and/or vesicles were made according to the procedure of Machesky²⁸ and then passed over the chip to examine binding.

Isothermal Titration Calorimetry (ITC)

ITC experiments were carried out on a Microcal VP-ITC instrument using Origin software to analyze the data. The WT profilin (131 µM, 0.4 mL) was titrated into a reservoir containing 1.8 mL of 30 µM PIP₂ vesicles. Vesicles were made as described above. Prior to the experiment both the protein and vesicles were dialyzed exhaustively into 10 mM tris, 40 mM KCl, pH 7.5 using 3500 MWCO dialysis tubing.

Binding Filtration Assay

This procedure has been modified from that of Lambrechts²⁹. PIP₂ vesicles were made as described above. Increasing concentrations were incubated with the WT protein in 10 mM tris, 40 mM KCl, 1 mM BME, pH 7.4 for 30 minutes on ice. Next the samples were subjected to centrifugation at 2000g for 2.5 minutes in a Millipore microcon filter with a 100 kDa MWCO. Then the filters were flipped over and centri at 1000g for 1 minute to collect any protein remaining on top. The assay was also done with the G4 PIP₂ dendrimer in the same way except a 50,000 MWCO filter was used and the samples were subjected to centrifugation at 3500g for 4 minutes. After centrifugation, all samples were brought to the same volume with buffer and 10 µL was taken to assay on a polyacrylamide gel (16% resolving, 5% stacking). To the sample, 10 µL of SDS loading dye (62.5 mM Tris-Cl, pH 6.8, 2% SDS, 10% glycerol, 0.01% bromophenol blue) was added and also 1 µL of either APH BHis (protein created in the lab, MW = 7550 Da) or PMSF treated bovine trypsinogen (1 mg/mL, Sigma) to use as a standard to account for gel loading errors. After running the gels at 170 V for 45 minutes, they were stained using a fluorescent SYPRO Ruby dye according to the procedure from the manufacturer³⁰ and imaged using a Typhoon 9210 (Amersham Biosciences). A green laser (532 nm) was used with a 610BP30 emission filter. Imagequant was then used to analyze the band intensities.

Synthesis of Biotinylated G1 PIP₂ mimic

*Biotinylated squarate tether*³¹ (**1**): A synthetic biotin tether was prepared according to the procedure of Nelson³². 3,4-diethoxy-3-cyclobutene-1,2-dione (586 µL, 3.96 mmol) was dissolved in 19.8 mL DMF. Biotin tether (443 mg, 0.99 mmol) was added slowly over 10 minutes and reaction was stirred under inert atmosphere at room temperature overnight. Reaction was concentrated in vacuo and purified via flash chromatography (100:1 CHCl₃/TEA to 400:50:1 CHCl₃/MeOH/TEA). The product was characterized using MALDI mass spectroscopy and one and two dimensional ¹H NMR (Yield: 53%, 298 mg, 0.522 mmol). ¹H NMR (D₂O) δ: 4.70-4.60 (m, 3 H), 4.60-4.52 (m, 1 H), 3.70-3.50 (br m, 14 H), 3.32-3.18 (m, 3 H), 2.99-2.90 (dd, 1 H), 2.75-2.68 (dd, 1 H), 2.25-2.15 (t, 2 H), 1.90-1.80 (m, 2 H), 1.80-1.45 (br m, 6 H), 1.45-1.30 (m, 5 H). MALDI-TOF: Calculated for C₂₈H₄₆N₄O₈S: 570.70; found (MH⁺): 571.41.

Biotinylated G1 PAMAM dendrimer (2): G1 PAMAM dendrimer (10 mg, 0.007 mmol) was reacted with **1** (3.4 mg, 0.006 mmol) in 250 μ L DMF. The reaction was stirred under inert atmosphere at room temperature overnight. Product was purified by reverse phase C¹⁸ HPLC (15-25% CH₃CN over 60 min gradient with 10 min hold in beginning at 10% CH₃CN, monitored at 280 nm). The product was characterized using MALDI mass spectroscopy and ¹H NMR (Yield: 36.4%, 5.1 mg, 0.003 mmol). ¹H NMR (D₂O) δ : 4.55-4.48 (m, 1 H), 4.35-4.30 (m, 1 H), 3.70-3.50 (m, 14 H), 3.50-3.45 (t, 2 H), 3.45-3.38 (t, 16 H), 3.36-3.30 (t, 2 H), 3.30-3.18 (br m, 10 H), 3.18-3.13 (t, 2 H), 3.12-3.02 (t, 16 H), 2.96-2.55 (br m, 36 H), 2.50-2.30 (br m, 20 H), 2.20-2.12 (t, 2 H), 1.90-1.75 (m, 2 H), 1.75-1.40 (m, 6H), 1.40-1.25 (m, 2 H). MALDI-TOF: Calculated for C₈₆H₁₆₄N₃₀O₁₉S: 1954.47; found (MH⁺): 1955.18.

Biotinylated G1 squarate PAMAM dendrimer (3): **2** (21 mg, 0.0107 mmol) was dissolved in 280 μ L DMF. 3,4-diethoxy-3-cyclobutene-1,2-dione (55.6 μ L, 0.376 mmol) and diisopropylethylamine (65.5 μ L, 0.376 mmol) were added to the reaction. The reaction was stirred at room temperature for 4 hours and then concentrated in vacuo. The mixture was then purified using Bio-Rad Bio-Gel P2 polyacrylamide size exclusion gel. The column was equilibrated in 20% ethanol and the sample was loaded in 500 μ L of 20% ethanol. Fractions were assayed with UV light to isolate the desired compound. The product was characterized by ESI mass spectroscopy and one and two dimensional ¹H NMR (Yield: 35%, 10.5 mg, 0.0037 mmol). ¹H NMR (D₂O) δ : 4.70-4.55 (m, 14 H), 4.55-4.50 (m, 1 H), 4.35-4.30 (m, 1 H), 3.70-3.45 (br m, 30 H), 3.45-3.15 (br m, 27 H), 3.10-2.25 (br m, 63 H), 2.22-2.12 (t, 2 H), 1.90-1.40 (m, 8 H), 1.40-1.25 (m, 23 H). ESI: Calculated for C₁₂₈H₁₉₂N₃₀O₄₀S: 2823.14; found: 2824.00.

Biotinylated G1 PIP₂ dendrimer (4): **3** (5 mg, 1.77 x 10⁻³ mmol) was dissolved in 110 μ L 0.1 M NaHCO₃ pH 9 with the previously prepared PIP₂ headgroup⁹ (14.6 mg, 0.0248 mmol). The reaction was stirred at room temperature for 6 days and monitored by

¹HNMR. The product was purified by dialysis (1000 MWCO) and is currently being characterized by ESI mass spectrometry and NMR.

Results and Discussion

The goals of my C500 project were to examine the binding interaction between the dendrimers and profilin and also to work on the synthesis of the biotinylated PIP₂ micelle mimic. Specifically I worked on investigating the binding between profilin and the G4 PIP₂ micelle mimic.

Surface Plasmon Resonance (SPR): Coupling of PI(4,5)P₂ headgroup analog

Initially I tried covalently coupling the PI(4,5)P₂ headgroup analog to a BIAcore CM4 sensor chip. The plan was to then flow WT profilin over the surface and monitor binding. The chip is composed of a stable carboxymethylated dextran matrix. The matrix was first activated using a mixture of NHS and EDC. Next the PIP₂ headgroup in water pH 5-6 was injected over the surface at a neutral pH according to the procedure of Prestwich²⁷. Binding studies showed that WT profilin did not bind to the chip. There are a few possible reasons for the WT protein's inability to bind. First, there may not have been any PIP₂ headgroup coupled to the chip for it to bind. Additionally, the few PIP₂ headgroups that may have been coupled to the chip might not have been in close enough proximity to one another to present a multivalent array to facilitate binding with profilin. Lastly, the whole lipid may be required for profilin binding. Additional attempts at coupling the headgroup proved problematic and it was found that regeneration conditions found by Prestwich²⁷ did not work in our hands. At this point, I decided to attempt coupling the protein instead of the PIP₂ headgroup using a different coupling method.

SPR: Coupling of HTN profilin

Modification of WT profilin afforded the protein with an N-terminal his₆x tag. I attempted to couple this protein to a BIAcore NTA sensor chip. This chip presented a carboxymethylated matrix immobilized with nitrilotriacetic acid (NTA). When coupled with Ni²⁺, chelation with the his-tagged protein takes place. Attempts to couple the HTN profilin showed the protein could be chelated to the surface of the chip, but was not stable at room temperature and leached off in a dissociative manner. Subsequent studies showed the protein to be stably chelated to the surface of the chip at 4°C. However, it was found that PIP₂ micelles did not bind to the protein. This can be seen in Figure 5.

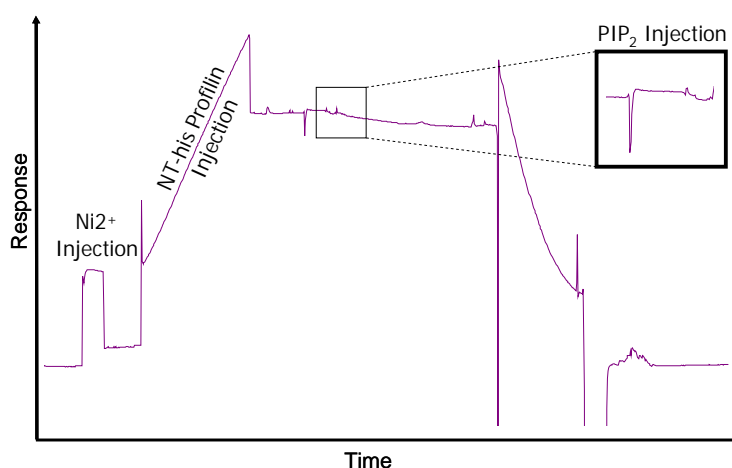


Figure 5. BIAcore sensorgram showing capturing of HTN profilin and subsequent injection of PIP₂ micelles.

After an injection of Ni²⁺, HTN profilin was immobilized onto the surface of the chip. Upon injecting PIP₂ micelles, no increase in response was seen which would indicate binding. This is not entirely surprising as one of the PIP₂ binding sites is postulated to be near the terminal ends of the protein²⁹. The introduction of a his-tag may have had a disruptive effect on binding.

SPR: Coupling of wildtype profilin

Next, I coupled the wild type protein to the surface of the CM4 chip using the EDC-NHS chemistry described above. Essentially the protein was coupled in a heterogeneous array through intrinsic amine groups. This method provided for an easy and quick immobilization of the protein and did in fact show promising binding data with

PIP₂ micelles. An example binding curve of wild type profilin with PIP₂ micelles is shown in Figure 6. The start of the injection of PIP₂ and the association phase is indicated by arrow 1 while the end of the injection and start of the dissociation phase is indicated by arrow 2.

Though it was easy to see initial binding results other aspects of the experiment proved difficult such as regeneration, protein, PIP₂ micelle stability, and reproducibility. A regeneration step is important for dissociating any remaining ligand from the surface of the chip to yield the original surface unharmed. Conditions must be found which are harsh enough to remove all of the bound PIP₂ micelles, yet are mild enough not to inactivate or permanently damage the wild

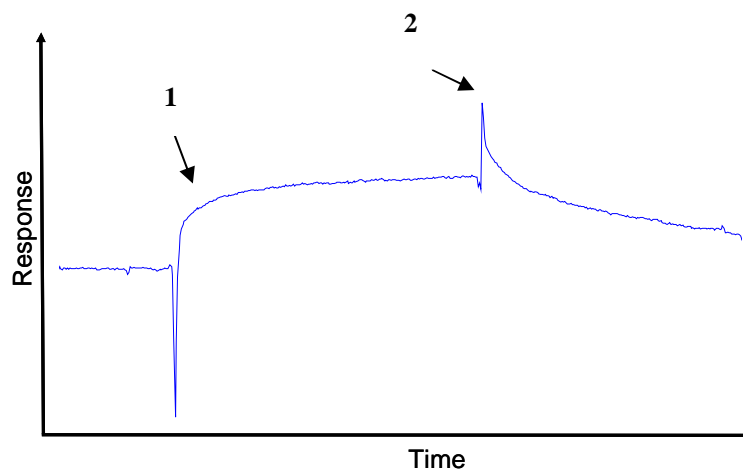


Figure 6. BIAcore sensorgram showing injection and binding of PIP₂ micelles to wild type profilin. Arrow 1 indicates the beginning of the injection and the association phase while the end of the injection and start of the dissociation phase is indicated by arrow 2.

type protein. The following chemicals were tested for their regeneration capabilities: urea, glycine, sodium hydroxide, guanidinium HCl, sodium chloride, and ethanolamine. Ultimately of these solutions tried, 1 M ethanolamine seemed to give the best results. Over multiple runs of binding and regeneration, the baseline level (amount of profilin immobilized) and the response level (amount of PIP₂ binding) remained essentially the same.

Though initial kinetic results were obtained in one experiment, fitting the data proved difficult and all available flow cells had been used. This would have altered the

available PIP₂ to the flow cell I was actually studying since some PIP₂ might have bound in other flow cells and also caused an apparently slower dissociation constant. Due to time constraints the experiment could not be repeated for a week. At this time it was found that the PIP₂ had gone bad and was no longer binding to the CM4 chip used or one which had been freshly derivatized with profilin. Upon obtaining new PIP₂, I still found diminished binding to the CM4 chip derivatized with profilin one month earlier, 150 RU initially vs. 15 RU one month later. After subjecting the chip to multiple cleaning steps involving the use of 1 mM dithiothreitol (DTT), I was able to regain approximately one third of the initial binding. Shown in Figure 7 is the regained binding after 5 injections of PIP₂ where the profilin on the chip has been exposed to DTT in between injections. It clearly shows that the more the chip is exposed to DTT, the more PIP₂ binding is regained. This would indicate that over time during storage profilin on the chip had undergone oxidation thereby preventing it from being able to bind to PIP₂ micelles.

Isothermal Titration Calorimetry (ITC)

As an alternative to the SPR experiment, we decided to attempt isothermal titration calorimetry (ITC) to examine binding. In this experiment, I titrated wild type profilin into vesicles composed of PIP₂/PC (1:5). For this experiment to work, the interaction of interest must have a large enough enthalpy of binding to be above the limiting sensitivity of the instrument. I found that the interaction of profilin with PIP₂

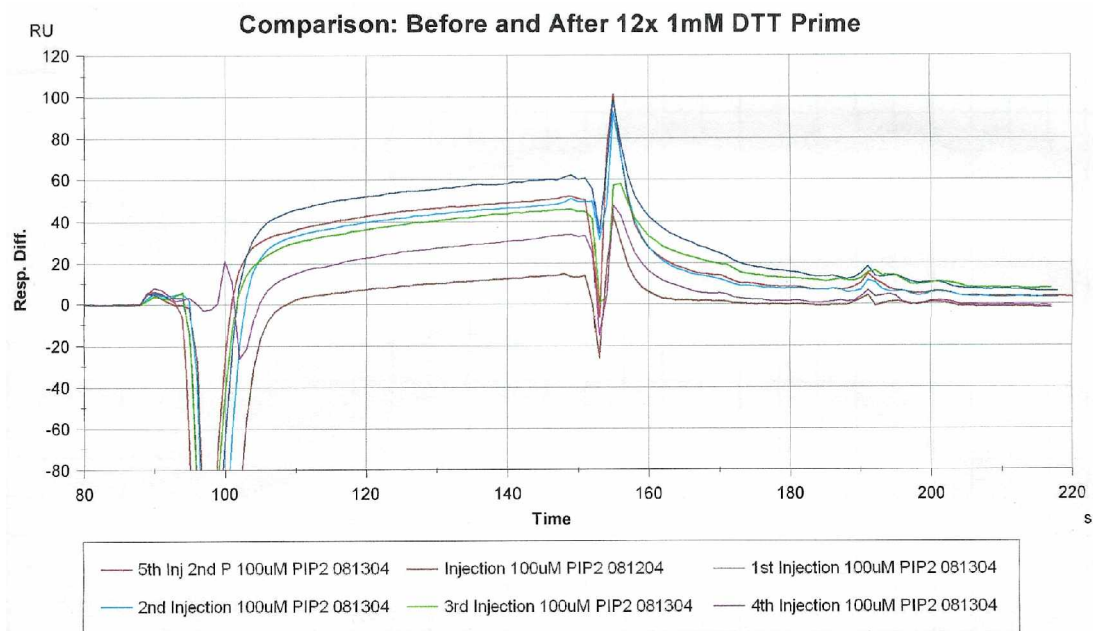


Figure 7. BIAcore sensorgram showing regained binding of PIP₂ micelles as profilin is repeatedly exposed to 1 mM DTT. Injection 1 081204 is prior to any DTT exposure while injections 1 081304 and 2 are after one DTT exposure, injections 3 and 4 are after 2 DTT exposures and injection 5 is after 3 DTT exposures.

was not in fact above this cut off for the concentrations I was studying. Initially a tris(hydroxymethyl) aminomethane buffer was used for the experiment which has a large enthalpy of ionization. If the binding between profilin and PIP₂ has a large enthalpy in the opposite direction, it would be possible for the enthalpy of the buffer to cancel out the enthalpy of the binding interaction. Therefore, the interaction was also examined in a cacodylate buffer. This buffer's enthalpy of ionization was nearly zero. However, similar results were obtained as previously. In order to get a better signal, it was determined that much higher quantities of PIP₂ and profilin would be needed.

Binding Filtration Assay

After spending large amounts of time on complicated techniques such as SPR and ITC, we sought to find a simpler, faster assay to examine binding. Based on an experiment done by Lambrechts, *et al*²⁹, we decided to study the binding between profilin with PIP₂ and the G4 dendrimer using a binding filtration assay. In this assay bound and free profilin were separated by a membrane with a MWCO under a centrifugal force

(Figure 8). After incubating the protein and dendrimer to allow for binding, the sample mixture is loaded into a centrifuge tube containing the dialysis membrane and spun for a specified amount of time at a predetermined speed. Any unbound profilin will be small enough to pass through membrane during centrifugation, while bound profilin will be larger than the membrane MWCO and will not pass

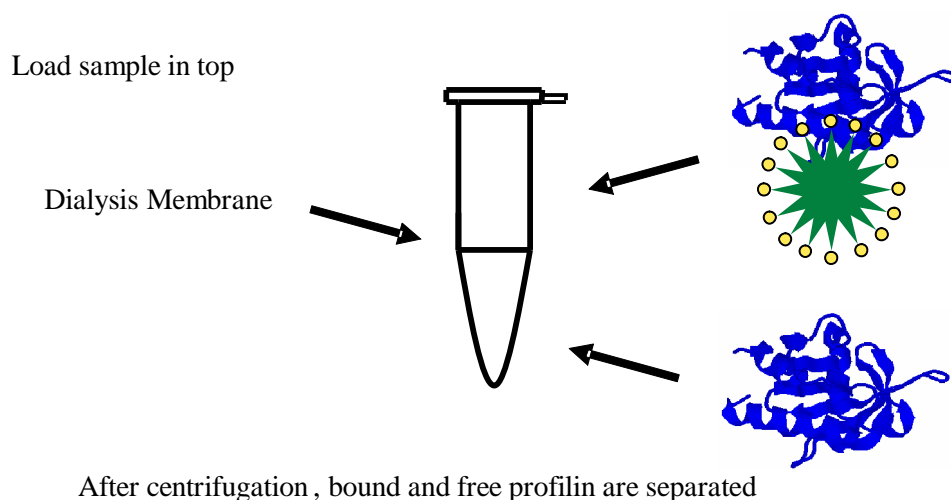


Figure 8. Demonstrates the filtration binding assay employed in our study of profilin-PIP₂ micelle mimic interaction.

through. By analyzing multiple samples with increasing amounts of dendrimer and by using SDS-PAGE, a binding curve can be obtained. Though this is not an equilibrium assay, our hopes were to attain a rough idea of the binding magnitude which then would later be refined by one of the more sophisticated methods (ex. SPR) for examining binding interactions.

Initially, I was not able to reproduce the data from the literature. I found that the time required to pass profilin through the membrane when in the presence of PIP₂/PC vesicles was longer than that reported²⁹. However, in the literature micelles of PIP₂ were used and a 30 kDa MWCO filter, whereas I was using PIP₂/PC vesicles and a 100 kDa MWCO filter. At this point, I began to focus more on the binding between profilin and the G4 PIP₂ micelle mimic and did not further optimize the assay for the profilin PIP₂

interaction. Experiments done by Sarah Richer indicated that profilin could pass through a 50 kDa MWCO filter and did not pass through a 30 kDa MWCO filter. Therefore, 50 kDa MWCO was used in all subsequent experiments with the G4 dendrimer. Initial optimization experiments indicated that spinning the samples at 7000 g for 4 min would efficiently transfer most profilin through when no dendrimer was present and also retain much of the profilin-dendrimer complex when dendrimer was present. By using these conditions, I was able to obtain reasonable data which can be seen in Figure 9. The left side of the figure shows that as the concentration of G4 is increased, the amount of free profilin decreases. The right side shows that as the concentration of G4 is increased the amount of bound profilin increases. These results give evidence for a binding interaction taking place.

From this data, binding curves were obtained shown in Figure 10. It clearly shows that as more G4 PIP₂ micelle mimic is added, the amount of bound profilin increases while the amount of free profilin decreases. However, upon further use of the filters, I could not repeat the fortuitous results seen in Figure 10. Later experiments indicated that the reproducibility between filters was very poor. Some filters would allow most profilin through with no G4 present, while other would hardly allow any through under the same conditions. A comparison of all experiments done thus far reveals the following graphs seen in Figure 11. It is clear from these graphs that there is much inconsistency involved with the different filters used for each trial.

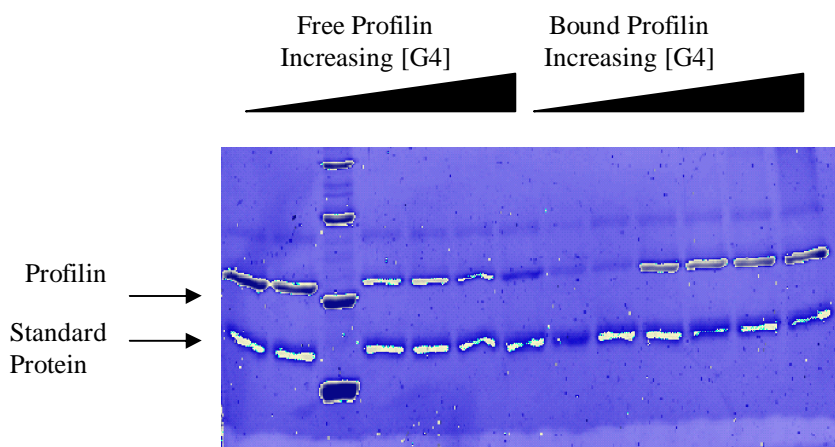


Figure 9. SDS-PAGE gel showing filtration binding assay results of profilin and G4 PIP₂ micelle mimic. Lanes 1 through 7 show free profilin which passed through the filter in the presence of increasing concentrations of G4. The last 6 lanes show bound profilin which remained on the top of the filter as the concentration of G4 was increased. The other band is a protein that was added to account for loading errors.

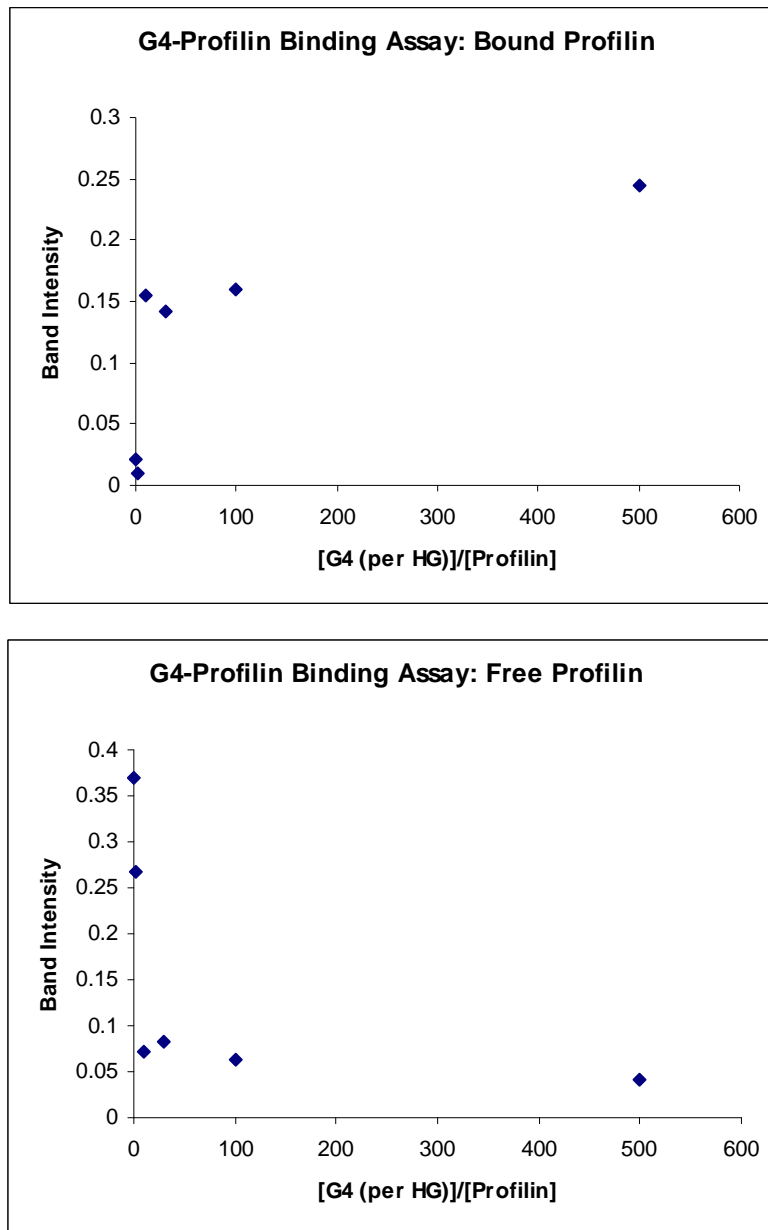


Figure 10. Binding curves obtained by analyzing band intensities on a Typhoon imager. The top curve shows that as G4 is added the amount of bound profilin increases, while the bottom curve shows that as G4 is added the amount of free profilin decreases.

As a last resort and attempt to eliminate error from filter to filter, our experimental evidence showed the error could be reduced by reusing one filter up to approximately 6 times. Upon trying this experiment with G4 and profilin, Sarah and I randomly chose 14 filters and passed profilin only through them. Next we ran polyacrylamide gels to isolate those filters which allowed the most profilin to pass in the flow through. Through this method we were able to find 2 filters. Next we proceeded with the binding assay examining 0-30 molar excess G4. However, upon running the gels, extra bands were apparent, either from contamination or degradation. Additionally there is clearly still protein present on the filters in the final wash between each sample. This indicates there could still be protein present on the filter for the next sample which could alter the data. This data set is represented by trial 5 in Figure 11. The data does seem to be consistent with the initial results obtained in trial 1. Subsequently, this method is currently being optimized through the use of 8 M urea between each sample to help aid in removal of all protein.

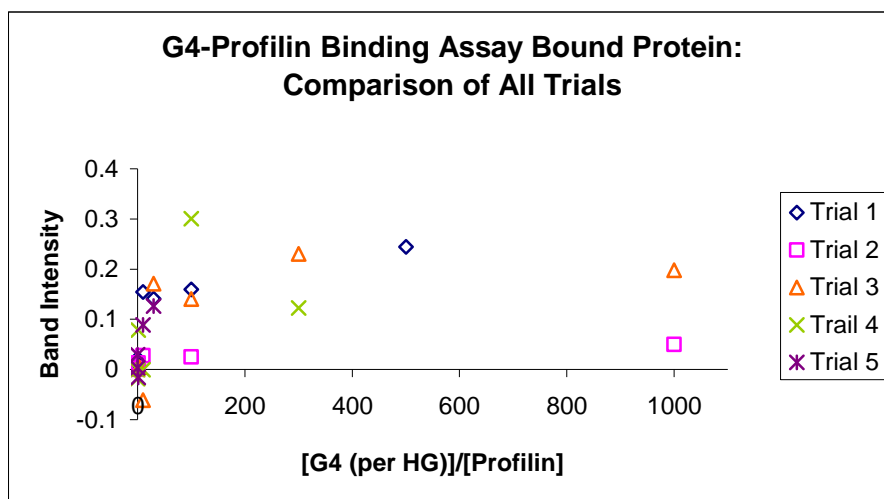


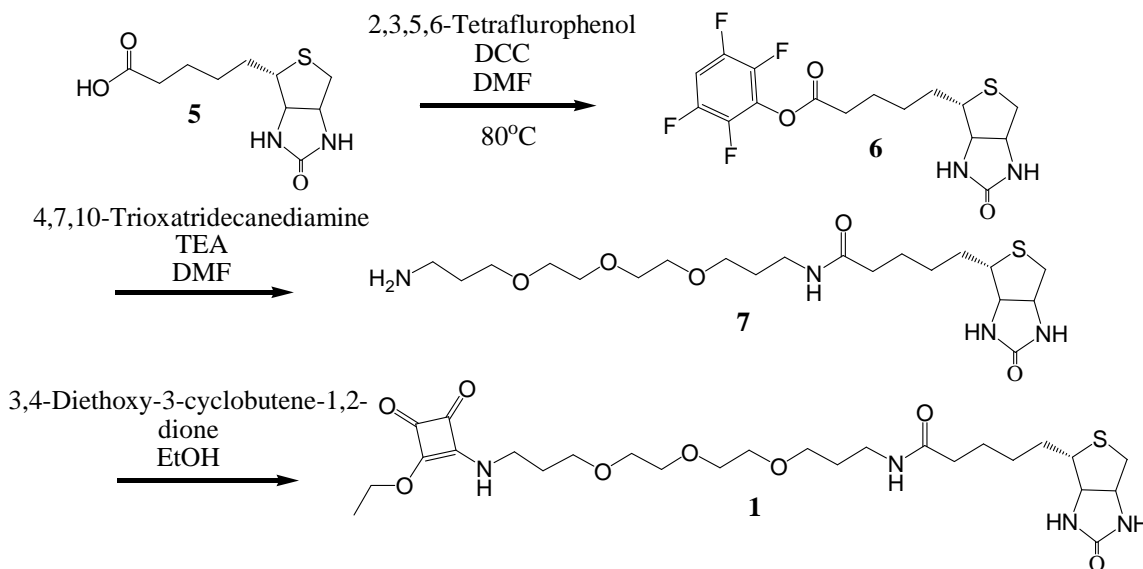
Figure 11. Graph showing overlay of all binding filtration assay results to date. The graph shows bound protein as a function of G4 concentration. Trial 1 represents the first set of data collected with this binding method, while trial 5 represents the most recent where one filter was reused for the entire binding assay.

Biotinylated G1 PIP₂ micelle mimic

Most of the work done thus far has only examined binding with the larger dendrimers (ex. G4). The binding filtration assay is appropriate for this size of dendrimer;

however, this method would not be expected to work for the smaller dendrimers (ex. G0, G1, G2). The combined size of the protein and smaller dendrimer would not be adequately large enough to remain on the top of the filter. For this reason, I have prepared a biotinylated G1 PIP₂ micelle mimic. This dendrimer contains a biotin tether and 7 PIP₂ headgroups. It is currently being characterized by ESI mass spectrometry and 1 and 2 dimensional ¹H NMR. This dendrimer can be immobilized on a streptavidin chip and used in SPR experiments to monitor binding with profilin. Additionally, other sizes of dendrimers can be made to contain the biotin moiety and will also be used for SPR experiments.

Initially, a biotin tether was synthesized as shown in Scheme 1. Chemistry through **7** was achieved using the methods of Nelson³². Subsequent addition of the squarate linker afforded **1**³¹. Additional steps gave the biotinylated G1 squarate PAMAM



Scheme 1. Overview of synthesis of the biotin squarate tether (**1**).

dendrimer (**3**). The ¹H NMR of **3** is shown in Figure 12 along with assignments made based on ¹H-¹H COSY NMR. The figure only shows ¼ of the dendrimer; the other ¾ not shown does not contain the biotin portion. The reaction of the previously prepared PIP₂ headgroup⁹ with **3** gave the biotinylated G1 PIP₂ micelle mimic (**4**) shown in Figure 13. This molecule is currently being characterized.

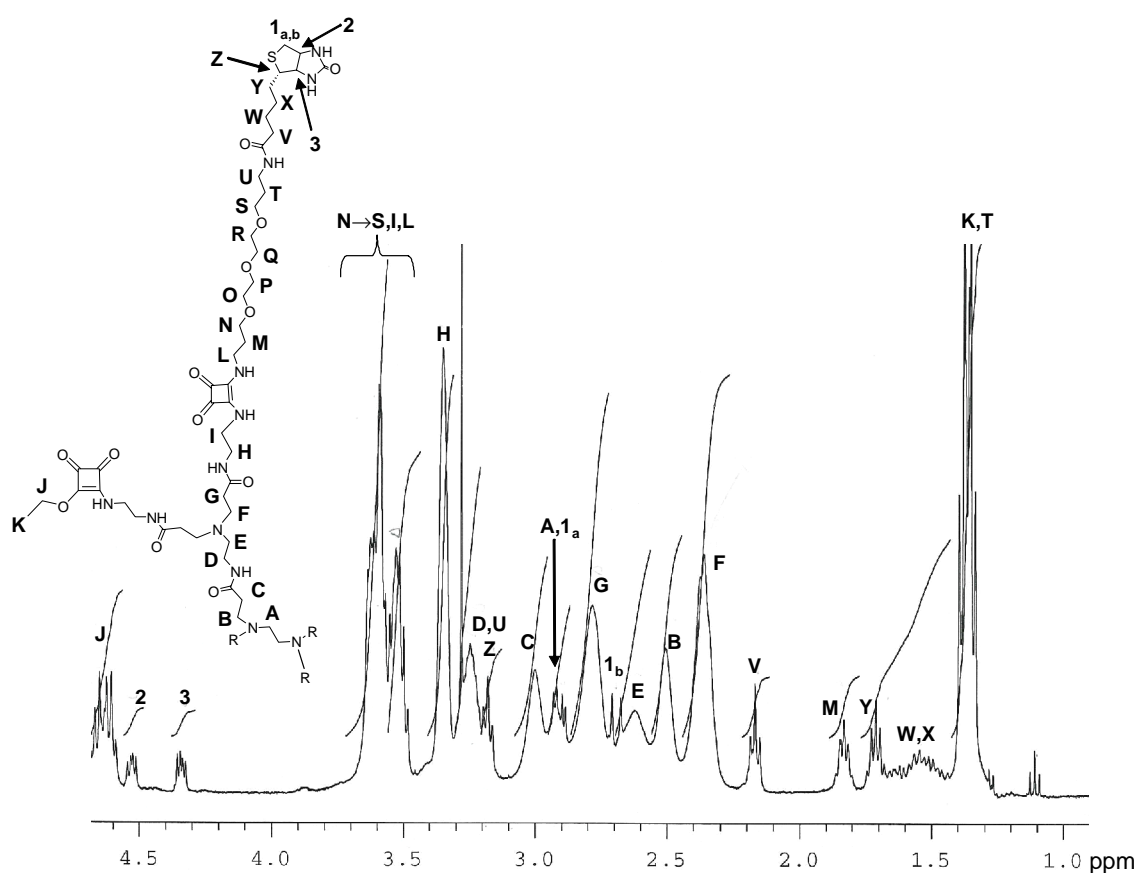


Figure 12. ^1H NMR of biotinylated G1 squarate PAMAM dendrimer (3). Assignments were made based on ^1H - ^1H COSY NMR.

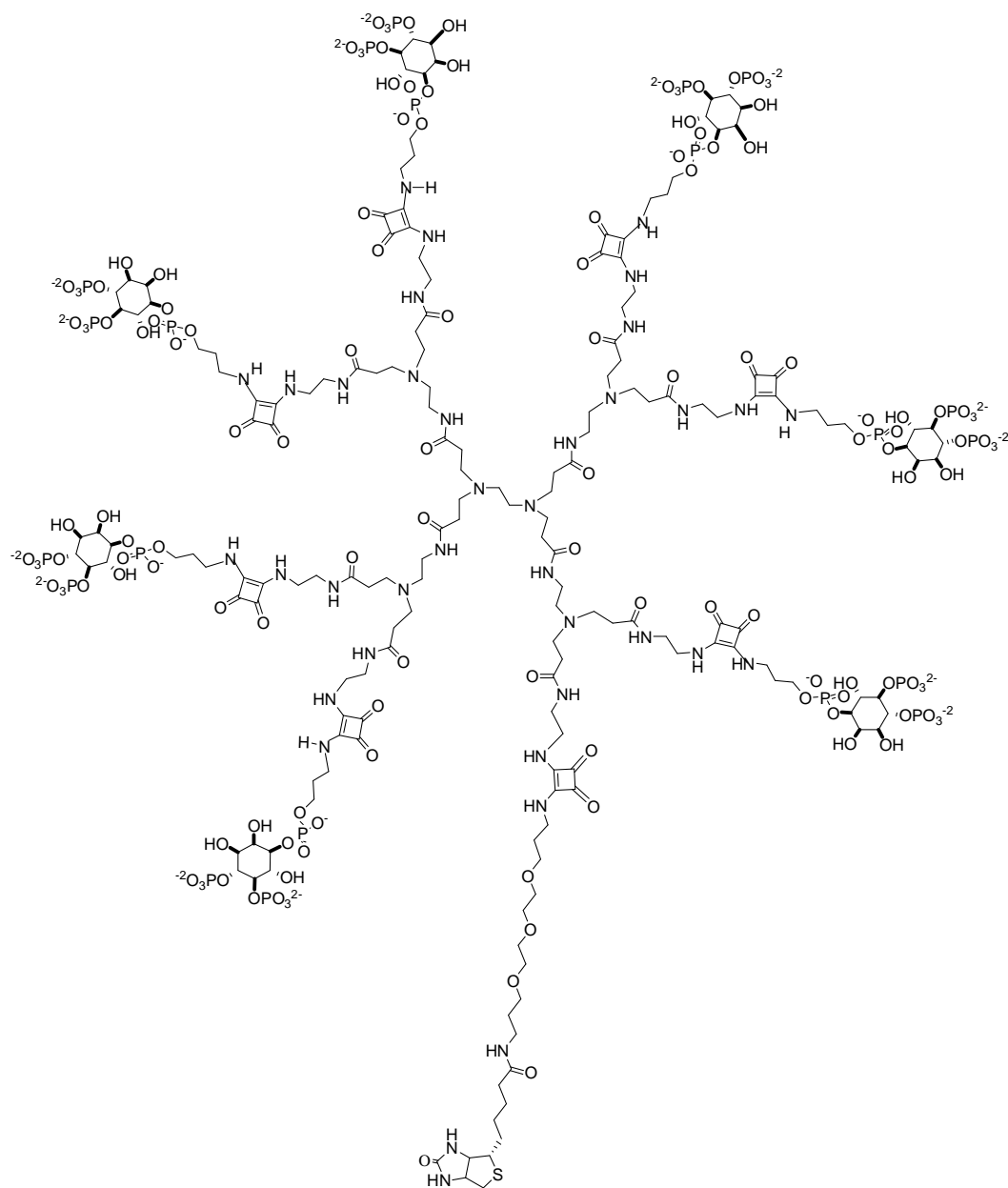


Figure 13. Structure of biotinylated G1 PIP₂ micelle mimic.

Conclusions and Future Work

In conclusion, I have begun to examine the binding interaction between PIP₂ and the PIP₂ G4 dendrimer with profilin by using SPR, ITC, and a binding filtration assay. Upon examining what has previously been done, several possible experiments could still be done to examine the binding between PIP₂ and profilin using SPR. Additional experiments would include the reexamination of the amine coupling of the wild type profilin. It is

possible to incorporate a running and storage buffer which includes 1 or 2 mM DTT. This would ensure longer stability of profilin when coupled to the chip. I also believe that previous regeneration conditions would still be applicable in this experiment. It might simply be best to derivatize the chip and carry out the binding experiments in a relatively short period of time, i.e. 1 or 2 days. Additional SPR experiments would involve the coupling of the biotinylated G1 PIP₂ mimic and evaluation of binding with profilin. Lastly the binding filtration assay can be repeated with the 8 M urea wash in between samples.

Reference List

1. Toker, A. Phosphoinositides and signal transduction. *Cell Mol. Life Sci.* **2002**, *59*, 761-779.
2. Janmey, P. Protein regulation by phosphatidylinositol lipids. *Chem. Biol.* **1995**, *2*, 61-65.
3. Yin, H. L.; Janmey, P. A. Phosphoinositide regulation of the actin cytoskeleton. *Annu. Rev. Physiol* **2003**, *65*, 761-789.
4. Ferrell, J. D. J.; Huestis, W. H. Phosphoinositide metabolism and the morphology of human erythrocytes. *J. Cell Biol.* **1984**, *98*, 1992-1.
5. Hagelberg C; Allan D Restricted diffusion of integral membrane proteins and polyphosphoinositides leads to their depletion in microvesicles released from human erythrocytes. *Biochem. J.* **1990**, *271*, 831-834.
6. DiNitto, J. P.; Cronin, T. C.; Lambright, D. G. Membrane recognition and targeting by lipid-binding domains. *Sci. STKE.* **2003**, *213*, 1-15.
7. Lemmon, M. A. Phosphoinositide binding domains. *Traffic* **2003**, *4*, 201-213.
8. Niggli V. Structural properties of lipid-binding sites in cytoskeletal proteins. *Trends Biochem. Sci.* **2001**, *26* (10), 604-611.
9. Webb, S. A. Synthesis and Characterization of Multivalent Mimics of Phosphatidylinositol-4,5-bisphosphate (PIP₂) Micelles. 2004.
10. Ostrander, D. B.; Gorman, J. A.; Carman, G. M. Regulation of profilin localization in *Saccharomyces cerevisiae* by phosphoinositide metabolism. *J. Biol. Chem.* **1995**, *270* (45), 27045-27050.
11. Goldschmidt-Clermont, P. J.; Machesky, L. M.; Doberstein, S. K.; Pollard, T. D. Mechanism of the interaction of human platelet profilin with actin. *J. Biol. Chem.* **1991**, *113* (5), 1081-1089.
12. Wittenmayer, N.; Jandrig, B.; Rothkegel, M.; Schluter, K.; Arnold, W.; Haensch, W.; Scherneck, S.; Jockusch, B. M. Tumor suppressor activity of profilin requires a functional actin binding site. *Mol. Biol. Cell* **2004**, *15* (4), 1600-1608.
13. Sohn, R. H.; Chen, J.; Koblan, K. S.; Bray, P. F.; Goldschmidt-Clermont, P. J. Localization of a binding site for phosphatidylinositol 4,5-bisphosphate on human profilin. *J. Biol. Chem.* **1995**, *270* (36), 21114-21120.

14. Chaudhary, A.; Chen, J.; Gu, Q. M.; Witke, W.; Kwiatkowski, D. J.; Prestwich, G. D. Probing the phosphoinositide 4,5-bisphosphate binding site of human profilin I. *Chem. Biol.* **1998**, 5 (5), 273-281.
15. Yu, F.-X.; Sun, H. Q.; Janmey, P.; Yin, H. L. Identification of a polyphosphoinositide binding sequence in an actin monomer-binding domain of gelsolin. *J. Biol. Chem.* **1992**, 267, 14616-14621.
16. Fedorov, A. A.; Magnus, K. A.; Graupe, M. H.; Lattman, E. E.; Pollard, T. D.; Almo, S. C. X-ray structures of isoforms of the actin-binding protein profilin that differ in their affinity for phosphatidylinositol phosphates. *Proc. Natl. Acad. Sci. U. S. A* **1994**, 91, 8636-8640.
17. Raghunathan, V.; Mowery, P.; Rozycki, M.; Lindberg, U.; Schutt, C. Structural changes in profilin accompany its binding to phosphatidylinositol, 4,5-bisphosphate. *FEBS Lett.* **1992**, 297 (1-2), 46-50.
18. Lassing, I.; Lindberg, U. Specific interaction between phosphatidylinositol 4,5-bisphosphate and profilactin. *Nature* **1985**, 314, 835-838.
19. Goldschmidt-Clermont, P. J.; Machesky, L. M.; Baldassare, J. J.; Pollard, T. D. The actin-binding protein profilin binds to PIP2 and inhibits its hydrolysis by phospholipase C. *Science* **1990**, 247 (4950), 1575-1578.
20. Machesky, L. M.; Goldschmidt-Clermont, P. J.; Pollard, T. D. The affinities of human platelet and *Acanthamoeba* profilin isoforms for polyphosphoinositides account for their relative abilities to inhibit phospholipase C. *Cell Regul.* **1990**, 1 (12), 937-950.
21. Mammen, M.; Seok-Ki, C.; Whitesides, G. M. Polyvalent Interactions in Biological Systems: Implications for Design and Use of Multivalent Ligands and Inhibitors. *Angew. Chem. Int. Ed. Engl.* **1998**, 37, 2754-2794.
22. Kitov, P. I.; Sadowska, J. M.; Mulvey, G.; Armstrong, G. D.; Ling, H.; Pannu, N. S.; Read, R. J.; Bundle, D. R. Shiga-like toxins are neutralized by tailored multivalent carbohydrate ligands. *Nature* **2000**, 403, 669-672.
23. Woller, E. K.; Cloninger, M. J. The lectin-binding properties of six generations of mannose-functionalized dendrimers. *Org. Lett.* **2002**, 4 (1), 7-10.
24. Tomalia, D. A.; Naylor, A. M.; Goddard III, W. A. Starburst Dendrimers: Molecular-Level Control of Size, Shape, Surface Chemistry, Topology, and Flexibility from Atoms to Macroscopic Matter. *Angew. Chem. Int. Ed. Engl.* **1990**, 29, 138-175.

25. Webb, S. A.; Stewart, N. K.; Belcher, L. J.; Mechref, Y.; Tomaszewski, J. W.; Novotny, M. V.; Oakley, M. G. Synthesis and characterization of synthetic PIP2 micelles. Unpublished Work, 2006.
26. Fedorov, A. A.; Pollard, T. D.; Almo, S. C. Purification, characterization and crystallization of human platelet profilin expressed in *Escherichia coli*. *J. Mol. Biol.* **1994**, *241*, 480-482.
27. Mehrotra, B.; Myszka, D. G.; Prestwich, G. D. Binding kinetics and ligand specificity for the interactions of the C2B domain of synaptogmin II with inositol polyphosphates and phosphoinositides. *Biochemistry* **2000**, *39*, 9679-9686.
28. Machesky, L. M.; Cole, N. B.; Moss, B.; Pollard, T. D. Vaccinia virus expresses a novel profilin with a higher affinity for polyphosphoinositides than actin. *Biochemistry* **1994**, *33* (35), 10815-10824.
29. Lambrechts, A.; Verschelde, J. L.; Jonckheere, V.; Goethals, M.; Vandekerckhove, J.; Ampe, C. The mammalian profilin isoforms display complementary affinities for PIP2 and proline-rich sequences. *EMBO J.* **1997**, *16* (3), 484-494.
30. Molecular Probes, I. d. t. SYPRO Ruby protein gel stain product information. 2005.
Ref Type: Pamphlet
31. Tietze, L. F.; Arlt, M.; Beller, M.; Glusenkamp, K.; Jahde, E.; Rajewsky, M. F. Squaric acid diethyl ester: A new coupling reagent for the formation of drug biopolymer conjugates. Synthesis of squaric acid ester amides and diamides. *Chem. Ber.* **1991**, *124*, 1215-1221.
32. Nelson, K. E.; et al. Surface characterization of mixed self-assembled monolayers designed for Streptavidin immobilization. *Langmuir* **2001**, *17*, 2807-2816.